Journal of Molecular Structure 1180 (2019) 378–391

Contents lists available at ScienceDirect

Journal of Molecular Structure

journal homepage: http://www.elsevier.com/locate/molstruc

ATR-FTIR analysis on the hydrogen bonding network and glycosidic bond of DC air plasma processed cellulose

S. Anitha [a, *], K. Vaideki [a], S. Prabhu [a], S. Jayakumar [b]

[a] Department of Applied Science, PSG College of Technology, Coimbatore, India
[b] PSG Institute of Technology and Applied Research, Coimbatore, India

ARTICLE INFO

Article history:
Received 22 August 2018
Received in revised form
26 November 2018
Accepted 4 December 2018
Available online 5 December 2018

Keywords:
DC air plasma process
Cotton fabric
Box-Behnken design
Langmuir probe analysis
Lateral order index and cellulose oxidation
Mean pore radius

ABSTRACT

The optimisation of DC plasma process towards maximising the fabric's hydrophilicity using Design-Expert 7.0.0 software has been reported in this paper. Out of various designs available, the Box-Behnken design was adopted for this purpose. The process parameters considered for optimisation were pressure of the gas (commercial grade air) used to produce plasma, DC current and the time for which the fabric was exposed to the plasma. These were keyed in as the three input parameters and the corresponding measure of hydrophilicity was fed as the response. Analysis of Variance (ANOVA) of the model and an associated discussion on the basis of Langmuir probe analysis, Physical analysis and ATR-FTIR analysis has been reported. The response predicted by the model was in good agreement with that obtained through experiment.

1. Introduction

Generally in any type of experiment the input process parameters play a vital role in improving the performance of the output. While analysing a process, experiments have to be performed in order to identify the level of the inputs to achieve a desired output. In several studies the input parameters are optimised by studying the effect of one single parameter on the output response keeping the other factors constant. This method of optimisation may cause errors, because the interaction of parameters is not taken in to account [1]. Further, this type of experimental procedure will involve mismanagement of time and material.

To overcome this problem many statistical techniques are developed to give the relationship between input parameters and output responses. The various methods that are commonly used for the optimisation process are analytic methods and Artificial Intelligence (AI) based techniques. Out of these techniques, Design of Experiment (DOE) is an experimental or analytical method that is commonly used to statistically signify the relationship between input parameters to output responses. In this analytical method, the systematic way of planning of experiments, collection and analysis of data is executed throughout the process.

The significance of DOE is the synergetic usage of mathematical and statistical techniques such as Regression, Analysis of Variance (ANOVA), Non-Linear Optimisation and desirability functions to optimize the parameters that makes this method a cost effective process. Various techniques were used in Design of Experiment and among them the most notably used are Response Surface Methodology, Taguchi's method and Factorial design.

Response surface methodology is a technique which uses factors with more than three levels to optimize the parameters and this way they can establish mathematical models. Central composite [2,3] Box–Behnken [2–4] and Doehlert designs [2–4] are among the principal response surface methodologies used in experimental design. In these models Central composite and Doehlert designs starts with the optimisation of two or more factors. For three factors, the Box-Behnken design offers certain advantage over central composite designs. Box-Behnken design is a special 3-level design that requires a fewer number of runs because it does not contain any points at the vertices of the cube region. These vertices points represent level combinations that are impossible to test because of physical process constraints.

The use of response surface methodology to optimize the plasma parameters has been reported earlier by several researchers. Meysam Baghery Borooj et al. [1] optimised the plasma

* Corresponding author.
E-mail address: vp.anitha@gmail.com (S. Anitha).

https://doi.org/10.1016/j.molstruc.2018.12.016
0022-2860/

process variables (treatment time, flow rate and power) using Response Surface Methodology (RSM) to improve the strength of carbon fibres/epoxy composite. It was found that quadratic model was suggested, and the individual effects of three variables and the interaction effects of treatment time-flow rate and treatment time-power shows the significant contribution on inter laminar shear strength. The same technique was employed to optimize the process parameters of corona discharge process using Box Behnken design of experiments by Dipayan Das et al. [5]. It was concluded that the applied voltage was the most influencing factor in deciding the surface potential of the electret media. The effect of Argon plasma treatment on various properties of polyester fabrics has been studied by Pandurangan Senthilkumar et al. [6] and the experiment parameters were optimised to yield better wettability and antibacterial properties. It was found that increase in both operating power and time and a decrease in distance between the electrodes had an influence on the said properties of the fabric. T. Karthik et al. [7] optimised the plasma treatment variables to improve the hydrophilicity of polylinen fabrics using Box–Behnken design. The optimum conditions for high wettability of the polylinen fabrics at a particular combination of treatment time, power and distance between the electrodes were achieved using the Box–Behnken design analysis. However, there are no articles that combine a discussion about the plasma species (viz ion density, electron density, electron temperature etc.) that are responsible for achieving optimised properties along with the statistical analysis.

Physical and chemical changes of the cellulose were studied to find the extent of surface modification after plasma treatment. Physical and chemical changes include etching, crystallinity changes and oxidation of the sample and these changes are responsible for increase in wicking ability of cellulose materials after plasma treatment. The plasma treatment enhances the formation of carboxylic acid group and creates the channel for water penetration [8].

Using, dynamic wicking test average pore radius of the plasma-treated fabrics was calculated to analyse the capillarity of this multiporous material. In several studies, the Fourier transform infrared spectroscopy (FTIR) technique was successfully applied to study the chemical changes viz., crystallinity changes and amount of oxidation of the cellulose. The lateral order (LOI) index, proposed by Nelson and O'Connor [9] is used to study the crystallinity changes. LOI is the ratio between the absorbance of 1429 cm^{-1} to the absorbance of 893 cm^{-1}. The peak at 1429 cm^{-1} corresponds to CH_2 stretching, the change in intensity or location of this peak related to alteration in C_6 environment of cellulose. The peak at 893 cm^{-1} corresponding to glycosidic C–*O*–C bond in the amorphous region of cellulose and it is sensitive to the interchain hydrogen bonds in the system and this peak represents weak parallel polarization. Hence an increase in this ratio represents an increase in lateral order in the cellulose unit cell whereas a decrease represents vice versa [9]. The peaks around 1700-1750 cm^{-1} were used to identify the functional groups that have been formed during oxidation process. Generally, oxidation of cellulose leads to functionalisation and a quantitative analysis of C=O stretching of these groups has been identified by infrared absorption spectra [10].

In the current study, Box-Behnken design (BBD) was employed to study the effect of plasma treatment on hydrophilicity of cotton fabric by using commercial grade atmospheric air as process gas. For the first time, results of Langmuir probe studies has been correlated with the physical and chemical changes and this study has been used to substantiate the Analysis of Variance (ANOVA) of Box Behnken design.

2. Experimental methods

2.1. Cotton fabric

The fabric used in the present study was a 100% pure cotton, finished, plain weave fabric with plain weave Ne 22's warp count and Ne 19's weft count with an EPI and PPI of 68 × 55, surface mass of 160 GSM and thickness of 0.36 mm. Cotton fabric was initially immersed in boiling water for an hour to remove starch and air dried. Finally the fabric was subjected to industrial pressing (Ironing).

2.2. DC plasma treatment

The DC plasma chamber and the electrodes were made of stainless steel. The dimensions of the chamber were 12″ in diameter, 50 cm in length. The volume of the chamber is 35,325 cm^3 with electrode area of 400 Sq. cm. The fabric sample of dimension 20 cm × 20 cm was made to float between electrodes, and the chamber was connected to the rotary pump (Hind Hivac). In the presence of the fabric, the minimum base pressure that can be attained was 0.2 mbar. The schematic diagram of plasma chamber was shown in Fig. 1.

The process parameters that can be varied during plasma treatment were electrode gap, process gas pressure, DC current, and plasma exposure time. Box Behnken design is a three factorial design where in, only three process parameters can be given as input. Hence, out of the above mentioned parameters the distance between the electrodes was fixed as 4 cm and the fabric was allowed to float at a distance of 2 cm between the cathode and the anode. Hence, the process gas pressure, DC current and plasma exposure time were the plasma process parameters that had to be optimised to attain maximum hydrophilicity.

Preliminary studies were carried out to set the range for pressure and current. Since the plasma chamber was evacuated to a base pressure of 0.2 mbar in the presence of fabric, the minimum pressure for which the plasma can be striked was 0.5 mbar. The rotary pump was switched on throughout the plasma treatment and the gas was pumped in through the needle valve to maintain the operating pressure and a continuous gas flow was ensured in the treatment zone. A maximum pressure of 1.5 mbar was attained when the needle valve was opened completely and this pressure

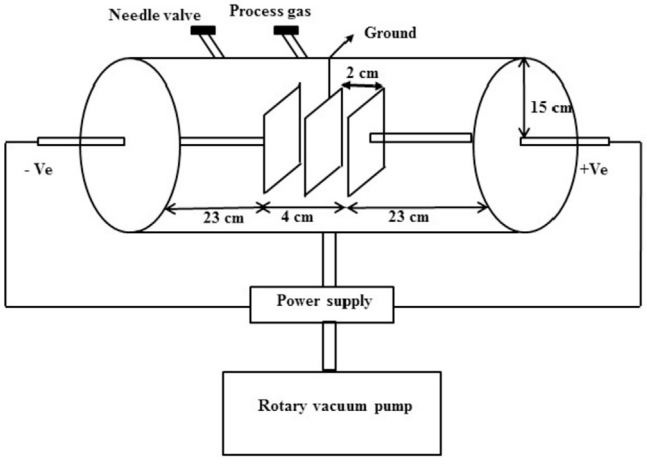

Fig. 1. Schematic diagram of DC plasma chamber.

was considered as the upper limit for the treatment.

The minimum current for which the plasma could be striked for a 0.5 mbar pressure was 5 mA and a sustained glow discharge was obtained upto 45 mA. When the current was increased beyond 45 mA, sparks were observed on the electrodes. Hence, 45 mA was set as the maximum current for the treatment. The time of treatment was set arbitrarily between 5 min and 25 min.

Prior to the plasma treatment the process gas was purged into the chamber for 2 min to fill the chamber.

2.3. Box-Behnken design

The optimisation of process parameters was done by three factors and three levels Box-Behnken design of experiment in combination with response surface methodology of analysis [11]. The uncoded (real) variables (factors) used were process pressure (X_1), DC current (X_2), Time of treatment (X_3) and these factors are illustrated in Table 1. The relationship between the coded and uncoded variable is given in the following equation.

$$x_1 = (X_1\text{-}1)/0.5 \quad (1)$$

$$x_2 = (X_2\text{-}25)/20 \quad (2)$$

$$x_3 = (X_3\text{-}15)/10 \quad (3)$$

where X_1, X_2, X_3 are the uncoded variables and x_1, x_2, x_3 are the coded variables.

Table 2 shows the complete design of 15 runs of experiments which includes 3 replicates at the centre point. The fabric samples were processed with plasma as per the combination of process parameters listed in Table 2. The hydrophilicity of these samples were assessed immediately without any time delay.

Table 1
Process variables and their levels.

Process variables	Levels		
	−1	0	+1
Pressure, P (mbar) **[X_1]**	0.5	1	1.5
DC current, I (mA) **[X_2]**	5	25	45
Time of treatment, t (min) **[X_3]**	5	15	25

Table 2
Coded and real variables.

Coded Variables			Real variables (Uncoded Variables)		
x_1	x_2	x_3	X_1	X_2	X_3
+1	0	+1	1.5	25	25
+1	0	−1	1.5	25	5
+1	1	0	1.5	45	15
+1	−1	0	1.5	5	15
0	−1	+1	1	5	5
0	1	−1	1	45	5
0	1	−1	1	45	25
0	0	0	1	25	15
0	0	0	1	25	15
−1	0	−1	0.5	25	5
0	0	0	1	25	15
−1	1	0	0.5	45	15
−1	0	+1	0.5	25	25
−1	−1	0	0.5	5	15
0	−1	+1	1	5	25

2.4. Assessment of hydrophilicity

The hydrophilicity of the untreated and DC plasma treated samples was measured by finding the wicking height using Dynamic wicking test (BS 4554) [12]. In this test, a strip of (2 cm × 20 cm) fabric is suspended vertically with its lower edge in contact with the distilled water. The rise in height of water (wicking height) was measured for different periods of time. The wicking height measured at 45 min was considered for the assessment of hydrophilicity. The measurements were taken for five strips of the same sample and the average wicking height was given as response to the respective experimental runs.

2.5. Statistical analysis of the design

The results of experiments were analyzed by response surface methodology using Design Expert software. The single as well as interaction effect of the process factors on the hydrophilicity of the cotton fabric were examined and the response of the experiment is represented in the form of equation (4).

$$Y = \beta_0 + \beta_1 x_1 + \beta_2 x_2 + \beta_3 x_3 + \beta_{12} x_1 x_2 + \beta_{13} x_1 x_3 + \beta_{23} x_2 x_3 + \beta_{11} x_1^2 + \beta_{22} x_2^2 + \beta_{33} x_3^2 \quad (4)$$

Where Y is the dependent variable i.e., the predicted response (Wicking height); $x_i (i = 1,2,3)$ refers to the independent variables (controlling factors); β_0 indicates the constant term; β_1, β_2, β_3 are the linear coefficients of the independent variables; β_{12}, β_{13}, β_{23} are the mixed quadratic coefficients; β_{11},β_{22},β_{33} indicates the squared quadratic coefficients.

Analysis of variance (ANOVA) gave the statistical analysis of the results. The significance of the model was given by F-test and the probability (P) value less than 0.05 was considered as the level of significance. Coefficient of regression (R^2) value predicts the Adequacy of the model.

2.6. Langmuir probe analysis

The cylindrical Langmuir probe (platinum wire of 0.18 mm diameter and 1 mm length) was placed between the electrodes for measurements. The probe construction was shown in Fig. 2.

Applied voltage was swept four times between −50 and +50 V and the current through the probe were measured using a micro ammeter and the readings were averaged. Fig. 3 shows the V–I plot for all the six sets of readings. From the Fig. 3, it is clear that there is no hysteresis disclosing the fact that at a certain location between

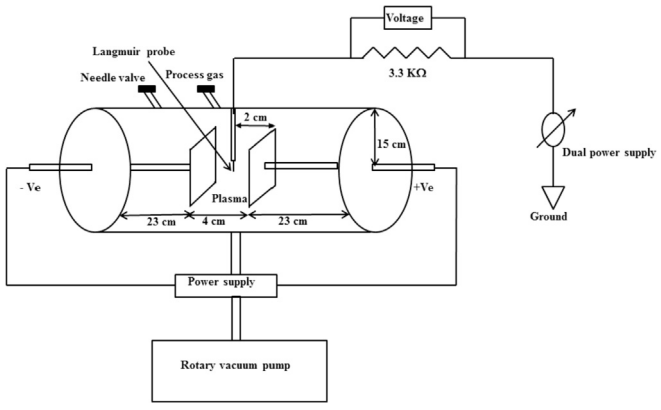

Fig. 2. Construction of Langmuir probe.

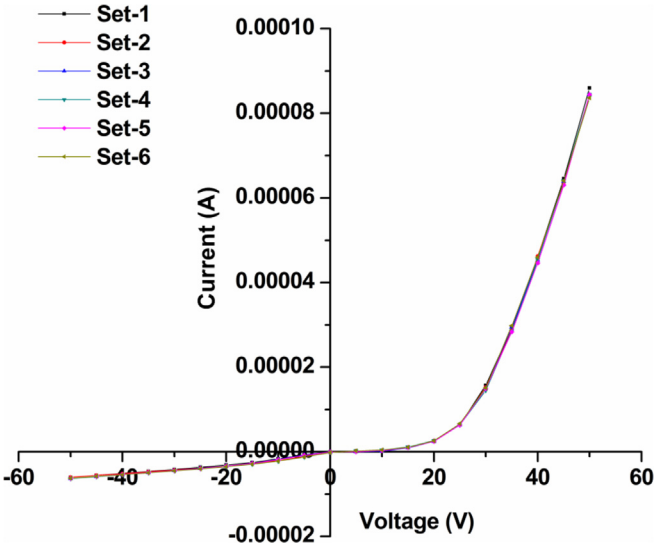

Fig. 3. V–I characteristics of Langmuir probe studies.

the electrodes, there is no fluctuation in the plasma species and it is almost constant with time though the rotary is switched on throughout the experiment. Therefore, to calculate the plasma parameters namely ion density, electron density, electron energy from the V–I plot, the average of six readings was considered.

The two theories namely, thin sheath analysis and Orbital Motion Limited collection theory describes the collection of charged particles by the probe. The appropriate theory depends on the parameters of the plasma, size and shape of the probe [13]. In thin sheath analysis, the size of the sheath is several times smaller than the radius of the probe (i.e) $r_p/\lambda_d \gg 1$, whereas in OML collection theory $r_p/\lambda_d < 1$. Chen specifies the conditions $r_p/\lambda_d > 10$ for thin sheath and $r_p/\lambda_d < 3$ for OML model [14].

In the present work, the debye length (λ_d) has been calculated from equation (8) and the values varied from 0.2 mm to 2 mm. Since, $r_p/\lambda_d < 3$ the requirements are satisfied for the applicability of the OML theory for various plasma process parameters. The ion density and electron temperature were calculated based on OML collection theory. The electron temperature was calculated using two different methods. First method is from the slope of semi-logarithmic plot of second derivative of the probe current (I_p) versus probe voltage (V_p) in the electron retarding region. Second method is from the slope of semi-logarithmic plot of I_e (electron current) versus probe voltage (V_p), where I_e is obtained by subtracting the ion component from total probe current. The calculated electron temperatures shows discrepancy between the methods, so the T_e value obtained from the first method is chosen.

The electron temperature (T_e) is determined using equation (5)

$$T_e = \frac{q}{ks} \tag{5}$$

where,

q is the electronic charge.
s is the slope.
k is the Boltzmann constant.

Laframboise method and Chen's method were employed to calculate ion density.

The Laframboise ion density was calculated using equation (6)

$$I_{sat} = 0.6qn_iA\left(\frac{2kT_e}{m_i}\right)^{\frac{1}{2}} \tag{6}$$

where,

I_{sat} = Ion saturation current.
q is the electronic charge.
n_i is the ion density.
A is the area of the probe.
k is the Boltzmann constant.
T_e is the electron temperature.
m_i is the mass of the ion.

Chen's ion density was calculated using equation (7)

$$J = \frac{I_{sat}}{2\pi LkT_e}\sqrt{\frac{m_i}{2n_i\varepsilon_o}} \tag{7}$$

Where,

I_{sat} = Ion saturation current.
n_i is the ion density.
L is the length of the probe.
k is the Boltzmann constant.
T_e is the electron temperature.
m_i is the mass of the ion.
ε_o is the permittivity of free space.

The debye length (λ_d) is determined using equation (8)

$$\lambda_d = \sqrt{\frac{\varepsilon_0 kT_e}{n_e q^2}} \tag{8}$$

where,

k is the Boltzmann constant.
T_e is the electron temperature.
n_e is the electron density.
q is the electronic charge.
ε_0 is the permittivity of free space.

2.7. Assessment of mean pore radius

Dynamic wicking test is used to determine the effective pore radius. The technique relies on describing liquid penetration kinetics inside a material by the Lucas Washburn equation (9). The Lucas Washburn equation is derived by combining the poiseuille's method for viscous flow and the Young-Laplace equation for capillarity [15]. Using Lucas Washburn equation, the average pore size of the fabric both before and after plasma treatment was calculated. The slope of the linear plot between L^2 and t provides the mean pore radius of the fabric.

$$L^2 = \left(\frac{R\gamma}{2\eta}\right)t \tag{9}$$

Where,

L– wicking height, R – mean pore radius, η – coefficient of viscosity of the liquid, γ – surface tension of the liquid, t – time taken for wicking.

The mean pore radius is calculated for untreated samples and plasma treated samples from Lucas Washburn equation. It was found to be 0.16 μm for untreated sample and it is compared with the plasma treated samples in the results and discussions section.

2.8. ATR-FTIR spectroscopy

The chemical changes due to the plasma treatment were analyzed using ATR-FTIR spectra. The spectra were recorded using a Perkin Elmer (Spectrum100) FTIR spectrometer in the range of 4000–500 cm^{-1} with a resolution of 1 cm^{-1}.

3. Results and discussions

3.1. Analysis of the model

The wicking height of untreated cotton fabric was measured and it was found to be 9.2 ± 0.067 cm. The fabric samples were treated using DC air plasma for the fifteen combinations of three process variables generated by the Box-Behnken experimental design. The average wicking height determined as per BS 4554 is fed in as the response to the respective experimental runs (Table 3) and the standard deviation and error of the average wicking height is reported in Table 4.

A detailed statistical analysis was carried out on the plasma treatment. Table 5 shows the "Sequential Model Sum of Squares" (technically "Type I") which explains how terms of increasing complexity contribute to the total model.

Adding the terms should reduce the error sum of squares and increase the regression sum of squares. The hierarchy of the models are linear vs Block, 2FI vs Linear, quadratic vs 2FI, Cubic vs Quadratic. Linear vs block shows the significant contribution of the linear terms (x_1, x_2 and x_3) to the model. 2FI vs Linear shows the significance of adding the two factor interaction terms (x_1x_2, x_2x_3 and x_1x_3) to the mean, block, and linear terms already in the model. Similarly, Quadratic vs 2FI show the importance of adding quadratic terms (x_{11}, x_{22} and x_{33}) to the all terms except cubic model. Cubic vs Quadratic gives the significance of the cubic terms beyond all other terms. Sum of squares is calculated by squared deviations from the mean value for each model. Degree of freedom is the number of model coefficients in the model.

F value is used to test the significance of adding new model terms to the terms already in the model. Significance of the term is tested after removal of remaining terms so F value should be high compared to other models. Based on response results and statistical summary table it is clear that for both the plasma treatments, quadratic model is suggested as the best fit. Compared to all the mathematical models, Quadratic model has highest order of polynomial with the significant additional terms of highest F value and lowest p-value. The highest F value shows the significance of quadratic model after removal of average, blocks and linear model, whereas the lowest p-value (Prob > F) indicates the improvement of model due to additional terms other than quadratic terms. From the table it is noted that, the cubic terms are aliased, so they are not useful for modelling purposes.

The "Lack of Fit Tests" (Table 6) explains how well the model fits the data and it gives the comparison between residual error and "Pure Error" from replicated design points.

If the model fails to explain the relationship between experimental factors and the response, it exhibits lack of fit. Further, when the interaction and quadratic term are not included in the model and results in large residuals while fitting the model, then the lack of fit occurs in the model. Sum of square in lack of fit table explains the portion of residual sum of squares that is due to the model not fitting the data. So the value should be low. The F value is the ratio between mean square of the model to the mean square of the error. The model should be selected such that it should have insignificant lack of fit i.e., model should have a high probability value ("Prob > F") greater than 0.1and low F value. The quadratic model, identified earlier as the suggested model, does not show significant lack of fit. Hence, lack of fit table also confirms that the quadratic

Table 3
Experimental factors and corresponding response.

Run	Factor 1 X_1:Pressure (mbar)	Factor 2 X_2:Current (mA)	Factor 3 X_3:Time (min)	Response Avg. Wicking height (cm)
1	1.5	45	15	12.90
2	1	25	15	12.80
3	1	5	25	9.46
4	1	5	5	11.26
5	0.5	25	5	12.94
6	1	45	5	12.30
7	1	45	25	12.70
8	0.5	45	15	13.34
9	1.5	25	25	11.80
10	0.5	25	25	13.13
11	1.5	5	15	10.50
12	1	25	15	12.20
13	1.5	25	5	13.30
14	0.5	5	15	11.28
15	1	25	15	12.26

Table 4
Standard deviation and Error for wicking height datas.

Run	Response Avg. Wicking height (cm)	Standard Deviation	Error (±)
1	12.90	0.04	0.02
2	12.80	0.09	0.04
3	9.46	0.05	0.03
4	11.26	0.83	0.41
5	12.94	0.10	0.06
6	12.30	0.12	0.07
7	12.70	0.04	0.02
8	13.34	0.13	0.07
9	11.80	0.05	0.03
10	13.13	0.05	0.03
11	10.50	0.05	0.03
12	12.20	0.14	0.07
13	13.30	0.13	0.07
14	11.28	0.16	0.08
15	12.26	0.14	0.07

Table 5
Statistical summary of the model predicted by Box-Behnken design of experiments.

Source	Sum of squares	DF	Mean square	F Value	p-Value Prob > F	
Mean vs Total	2212.39	1	2212.39			
Linear vs Mean	11.48	3	3.83	6.62	0.0081	
2FI vs Linear	2.05	3	0.68	1.27	0.3498	
Quadratic vs 2FI	**4.08**	**3**	**1.36**	**29.72**	**0.0013**	**Suggested**
Cubic vs Quadratic	0.022	3	7.458E-3	0.072	0.9695	Aliased
Residual	0.21	2	0.10			
Total	2230.23	15	148.68			

Table 6
Lack of fit tests.

Source	Sum of squares	DF	Mean square	F Value	p-Value Prob > F	
Linear	6.15	9	0.68	6.62	0.1381	
2FI	4.11	6	0.68	6.62	0.1370	
Quadratic	**0.022**	**3**	**7.458E-3**	**0.072**	**0.9695**	**Suggested**
Cubic	0.000	0				Aliased
Pure Error	0.21	2	0.10			

model best fits the response.

Model Summary Statistics is yet another analysis which confirms the validity of suggested model for the input response. Table 7 provides the Model Summary Statistics which gives the standard deviation, correlation coefficient and Predicted residual error sum of squares (PRESS) value.

These parameters play an important role in determining the best mathematical model for the response and the values present the variety of goodness of fit. The standard deviation value estimates the deviation of error in the design and the model therefore should exhibit low standard deviation (SD). R-Squared value (multiple correlation coefficients) denotes the correlation between the observed and predicted responses. For the best model the difference in responses should be small or unbiased, so that the data is fitted onto the regression line. There are certain limitations with the R squared term i.e., it cannot determine whether the coefficient and predictors are biased and it cannot predict whether the model is adequate. To overcome this problem, adjusted R squared term is used. Adjusted R-squared is the modified version of R-squared where it compares the explanatory power of regression models that contains different number of predictors. If too many predictor is added to the model, R squared value increases and will lead to the over fitting of the model. But the adjusted R squared value increases only if that added predictor improves the model and hence it explains the adequacy of the model. It is evident from the Table 7 that except for cubic and quadratic model all the source have lower R^2 and adj R^2 values which means that it will not fit the experimental data. Even though cubic model has higher R^2 value than quadratic model, the quadratic model obviously becomes the suggested one because the cubic model is aliased, which means the effects of each process variables that cause different signals become indistinguishable [16].

Predicted R-squared term explains how well the model predicts responses for new observation. This value is calculated by

Table 9
Wicking height of plasma treated fabrics with experimental, predicted response values and error.

Run	X_1	X_2	X_3	Experimental	Predicted	Error
1	1.5	45	15	12.90	12.89	0.01
2	1	25	15	12.80	12.43	0.37
3	1	5	25	9.46	9.37	0.09
4	1	5	5	11.26	11.24	0.02
5	0.5	25	5	12.94	12.99	−0.05
6	1	45	5	12.30	12.31	−0.01
7	1	45	25	12.70	12.76	−0.06
8	0.5	45	15	13.34	13.34	0.00
9	1.5	25	25	11.80	11.75	0.05
10	0.5	25	25	13.13	13.14	−0.01
11	1.5	5	15	10.50	10.57	−0.07
12	1	25	15	12.20	12.43	−0.23
13	1.5	25	5	13.30	13.30	0.00
14	0.5	5	15	11.28	11.21	0.07
15	1	25	15	12.26	12.43	−0.17

Table 7
Model summary statistics.

Source	Std.Dev.	R-Squared	Adjusted R-Squared	Predicted R-Squared	PRESS	Adequate Precision value	
Linear	0.76	0.6434	0.5462	0.2618	13.17		
2FI	0.73	0.7582	0.5768	−0.1808	21.06		
Quadratic	**0.21**	**0.9872**	**0.9640**	**0.9539**	**0.82**	**22.589**	**Suggested**
Cubic	0.32	0.9884	0.9189		+		Aliased

Table 8
Analysis of variance for the Quadratic model.

Source	Sum of Squares	df	Mean Square	F Value	p-value Prob > F	
Model	17.61	9	1.96	42.71	0.0003	Significant
A-Pressure	0.59	1	0.59	12.85	0.0158	Significant
B-Current	9.90	1	9.90	216.15	0.0001	Significant
C-Time	0.99	1	0.99	21.55	0.0056	Significant
AB	1.000E-2	1	1.000E-2	0.22	0.6600	Not Significant
AC	0.71	1	0.71	15.59	0.0109	Significant
BC	1.32	1	1.32	28.87	0.0030	Significant
A^2	0.81	1	0.81	17.58	0.0085	Significant
B^2	2.99	1	2.99	65.35	0.0005	Significant
C^2	0.043	1	0.043	0.94	0.3771	Not Significant
Residual	0.23	5	0.046			
Lack of Fit	0.022	3	7.458E-3	0.072	0.9695	Not Significant
Pure Error	0.21	2	0.10			
Cor Total	17.84	14				

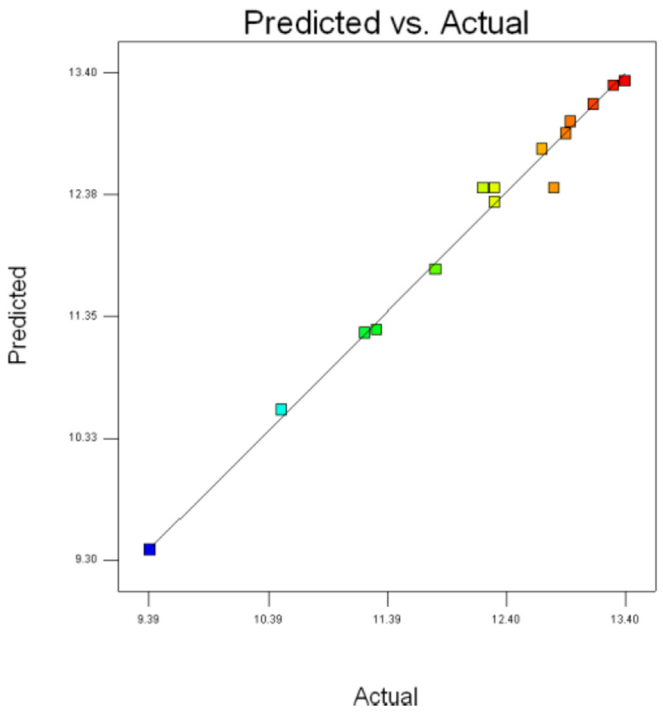

Fig. 4. Predicted and actual values DC air plasma treatment.

estimating the regression equation after removal of each observation from data set. Predicted Residual Error Sum of Squares (PRESS) value represents the fitness of the model with each design point. For a model to have better predictive ability, it should exhibit low "PRESS" value. PRESS value prevents over fitting of the model and this value is calculated using observations not included in the model estimation. Compared to all the models, it is evident from the Table 7 that quadratic model exhibits higher Predicted R^2 with low PRESS value because the quadratic model is selected to fit the

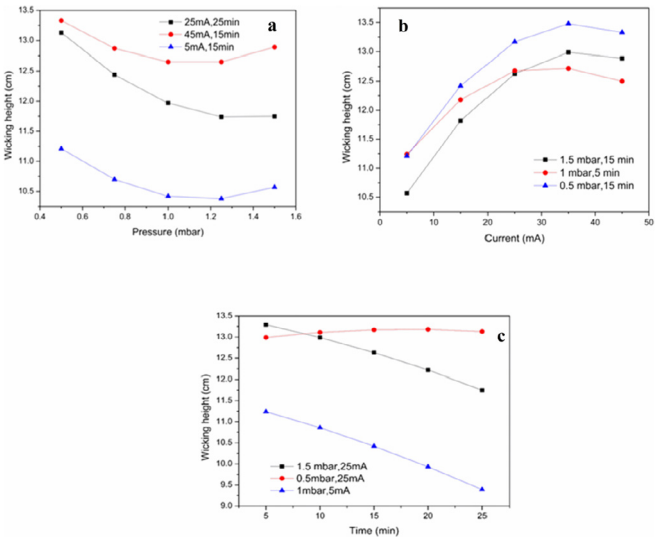

Fig. 6. One factor interaction of the variables on wicking height for DC air plasma treatment.

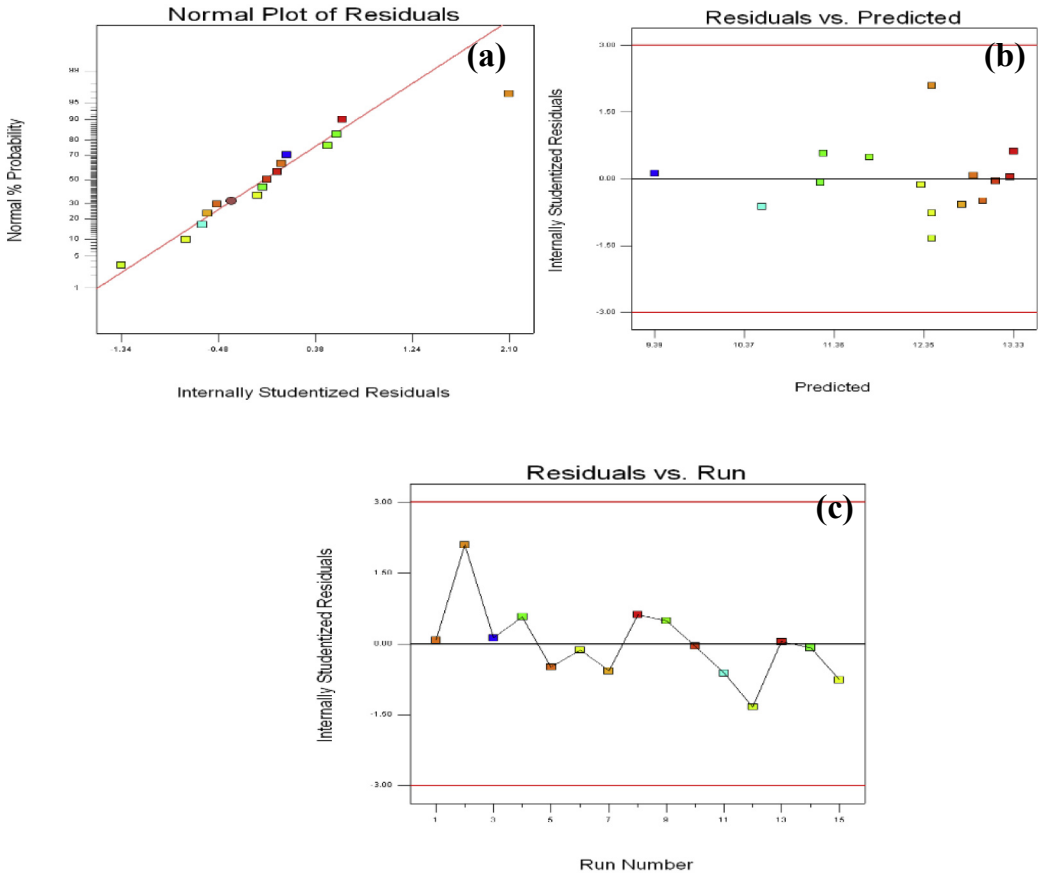

Fig. 5. Diagnostic plots for wicking height.

experimental data for DC air plasma treatment. Similarly the other parameter that confirms the model's significance is adequate precision which is a measure of the range in predicted response relative to its associated error [17]. The adequate precision values (i.e. signal to noise ratio) of wicking height is found to be 22.589 for DC air plasma treatment. The fact that the values above 4 states that the model could be used with in the region of operation.

3.2. ANOVA (analysis of variance)

The significance of the model is given by analysis of variance (ANOVA). The ANOVA in this case confirms the adequacy of the quadratic model (the Model Prob > F is less than 0.05). The ANOVA for quadratic model is given in Table 8, the results confirm that the model agrees well for the plasma treatment with the F value of 42.61 and p-value of 0.0003.

A Prob > F (p-value) lower than 0.05 shows the model is significant, and a value greater than 0.10000 indicates that the model is not significant [16]. It can be observed from Table 8 that the single effect of pressure, DC current and time, the quadratic effect of pressure, DC current and the interaction effect of pressure and current on time are found to be statistically significant.

The regression equation generated to relate the response (wicking height) with the variables is given in equation (10).

$$y = +12.26633 - 3.13667X_1 + 0.12005\,X_2 + 9.875E\text{-}3\,X_3 + 5E\text{-}3\,X_1X_2 - 0.0845\,X_1X_3 + 2.87500E\text{-}003\,X_2X_3 + 1.86833\,X_1^2 - 2.25104E\text{-}003\,X_2^2 - 1.07917E\text{-}003X_3^2 \quad (10)$$

Where y denotes the predicted wicking height of DC air plasma treated cotton fabric and X_1, X_2, X_3 are the process variables namely pressure, DC current, time of treatment respectively. The predicted

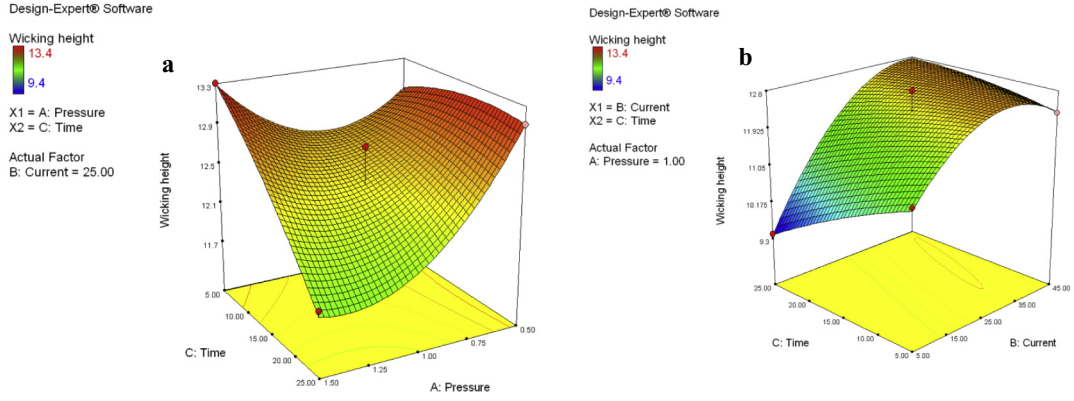

Fig. 7. Effect of simultaneous variation in a) gas pressure & exposure time b) DC current & exposure time on wicking height.

Table 10
Langmuir probe analysis of process parameters.

Process parameters				Langmuir probe analysis- Fixed current and Exposure time		
I (mA)	T (min)	P (mbar)	WH (cm)	n_i (ions/m^3) Laframboise method	n_i (ions/m^3) Chen method	T_e(eV)
5	15	0.5	11.28	1.33E15	0.71E15	8.48
5	15	1.5	10.50	4.99E15	0.10E15	8.29
25	25	0.5	13.13	4.78E15	0.43E15	7.72
25	25	1.5	11.80	5.93E15	0.93E15	5.11
45	15	0.5	13.34	7.15E15	0.66E15	6.83
45	15	1.5	12.90	8.77E15	1.25E15	2.55
Process parameters				**Langmuir probe analysis-Fixed pressure and Exposure time**		
P (mbar)	**T (min)**	**I (mA)**	**WH (cm)**	**n_i (ions/m^3) Laframboise method**	**n_i (ions/m^3) Chen method**	**T_e(eV)**
0.5	15	5	11.28	1.33E15	0.71E15	8.48
0.5	15	45	13.34	7.15E15	0.66E15	6.83
1	5	5	11.26	3.68E15	0.13E15	6.43
1	5	45	12.30	8.09E15	0.76E15	5.31
1.5	15	5	10.50	4.99E15	0.10E15	8.29
1.5	15	45	12.90	8.77E15	1.25E15	2.55
Process parameters				**Langmuir probe analysis-Fixed pressure and Fixed current**		
I (mA)	**P (mbar)**	**T (min)**	**WH (cm)**	**n_i (ions/m^3) Laframboise method**	**n_i (ions/m^3) Chen method**	**T_e(eV)**
25	0.5	5	12.94	4.78E15	0.43E15	7.72
25	0.5	25	13.13	4.78E15	0.43E15	7.72
5	1	5	11.26	3.68E15	0.13E15	6.43
5	1	25	9.46	3.68E15	0.13E15	6.43
25	1.5	5	13.30	5.93E15	0.93E15	5.11
25	1.5	25	11.80	5.93E15	0.93E15	5.11

Table 11
Physical and chemical analysis of process parameters.

Process parameters			Physical and chemical analysis				
I (mA)	T (min)	P (mbar)	WH (cm)	Mean pore radius (μm)	LOI		
					BT	AT	ΔLOI
5	15	0.5	11.28	0.29	0.67	0.50	0.17
5	15	1.5	10.50	0.21	0.60	0.59	0.01
25	25	0.5	13.13	0.31	0.60	0.67	−0.07
25	25	1.5	11.80	0.29	0.75	0.52	0.23
45	15	0.5	13.34	0.35	0.83	0.33	0.50
45	15	1.5	12.90	0.30	0.64	0.43	0.21
Process parameters			**Physical and chemical analysis**				
P (mbar)	**T (min)**	**I (mA)**	**WH (cm)**	**Mean pore radius (μm)**	**LOI**		
					BT	**AT**	**ΔLOI**
					0.83	0.33	0.50
1	5	5	11.26	0.25	0.32	0.25	0.07
1	5	45	12.30	0.30	0.60	0.40	0.20
1.5	15	5	10.50	0.21	0.60	0.59	0.01
1.5	15	45	12.90	0.30	0.64	0.43	0.21
Process parameters			**Physical and chemical analysis**				
I (mA)	**P (mbar)**	**T (min)**	**WH (cm)**	**Mean pore radius (μm)**	**LOI**		
					BT	**AT**	**ΔLOI**
					0.60	0.67	−0.07
5	1	5	11.26	0.25	0.32	0.25	0.07
5	1	25	9.46	0.20	0.75	0.67	0.08
25	1.5	5	13.30	0.36	0.58	0.56	0.02
25	1.5	25	11.80	0.29	0.75	0.52	0.23

response (wicking height) for fifteen samples are obtained from the equation and results are tabulated along with the experimental values. The difference in experimental and predicted values are stated as the error value in Table 9 and it is represented graphically in the Fig. 3.

Fig. 4 reveals that the variation between experimental (actual) and predicted response is linear with a slope of almost 1 which indicates that the experimentally observed values for the wicking height are in close agreement with the predicted values. A similar result was observed by Karthik et al., 2013 [7], in which it was reported about the effect of plasma parameters on improvement of wettability of polylinen fabric. Comparatively in this study, residuals are even much more closer to the diagonal line meaning that the calculated error between the actual and predicted value is quite low resulting in the adequacy of the model.

3.3. Diagnosis of the statistical properties of the model

Residual analysis is essential to investigate the goodness of the fit for the proposed model and to confirm that the assumptions for the ANOVA are met. The first step is the analysis on normal probability plot of the residuals which is given in Fig. 5(a).

Normal probability plot indicates whether the residuals follow normal probability distribution [18]. The normal probability plot should be linear; a non linearity in the data points indicates non normality in the error pattern. Fig. 5(a) reveals that the maximum number of points corresponding to wicking height lies on the straight line which infers that response data provided the relevant analysis. Fig. 5(b) depicts the plot of studentized residuals with predicted values. The nature of the plot should not follow megaphone shape instead it should be scattered which is the case in this study. Most of the points lie closer to the zero axis which indicates the absence of constant error. If any data point falls directly on the estimated regression line then it has a zero residual value. Fig. 5 (b) reveals that there are no actual data point deviated from the predicted value by the model (outliers) since all the residuals fall in to the basic random pattern. If there is any observation regarding the presence of the outlier then the plot will get deviated from the random pattern. These characteristics of the plot suggest the suitability of the simple linear regression model. The graphical representation of studentized variable versus order of experimental run is shown in Fig. 5(c). The random scattering of points indicate the absence of lurking variables for wicking height, which infers that the true relationship between the variables are not hidden [19].

3.4. ATR-FTIR analysis and dynamic wicking studies with reference to Langmuir probe studies

The analysis of variance of the quadratic model suggests that the variation in the factors X_1, X_2, X_3 individually has a significant effect on the hydrophilic property of the cotton fabric in DC air plasma treatment. Hence the effect of each individual factor namely gas pressure, DC current and exposure time for specific combinations of other two parameters on the wicking height is illustrated in Fig. 6(a–c) and the effect of simultaneous variation in gas pressure and exposure time for a constant current and simultaneous variation of DC current and exposure time at a fixed gas pressure on the response is presented in Fig. 7(a and b).

For three combinations of fixed current and exposure time, the effect of pressure on wicking height is illustrated in Fig. 6(a). The points in the plot were obtained by fitting the appropriate parameter values in the regression equation (9). The general observation is that the wicking height decreases and finally saturates with increase in pressure. A deeper analysis on the variation in

wicking height can be performed based on the knowledge of plasma species (ions, radicals, electrons etc.) present and their respective density and energy. Hence, DC air plasma was probed using single Langmuir probe for the combination of process parameters given by the Box-Behnken design. The Langmuir probe data is presented in Table 10.

It is noted from the table that, Laframboise OML ion density exceeds by the factor of 10–15 than corrected ion density from Chen's radial motion theory, the reason may be due to collisions with in the sheath [20]. Minimum threshold electron energy of 7 eV and 24.3 eV is required for electron impact dissociation of oxygen and nitrogen molecules respectively to produce oxygen and nitrogen atoms [21]. Once the atoms are produced, electron energy of 13.6 eV–5 eV is sufficient to trigger processes such as electron impact ionization of oxygen atom and molecule, ionization of Van der Waals molecules, ionization of low lying terms of oxygen atoms and dissociative electron attachment to generate positive and negative oxygen ions [21,22]. Whereas, electron energy of 14 eV–16 eV is required for generation of nitrogen ions [21]. From Table 10 it can be noted that the energy of electrons is sufficient to generate various oxygen ions but lower to produce nitrogen ions. Hence, the plasma generated would invariably possess higher concentration of plethora of oxygen species.

It is evident from Table 10, that irrespective of the combination of DC current and exposure time, even though the ion density increases with pressure wicking ability of the samples decreases with pressure. This can be attributed to the decrease in mean free path of the particles with increase in pressure as shown in Table 11. The mean free path of the chemically active species in the gas phase is lesser than the distance between the fibers that forms the thread [23]. Hence forth, the active plasma species will have less opportunity to reach the reaction site on the fiber surface supressing the effective surface modification thus decreasing the wicking ability.

The wicking ability of a cotton sample depends predominantly on the polar functional groups present in cotton cellulose and the average pore radius which influences the capillarity of the sample. The energetic charged particles present in the plasma upon interaction with the fabric modify the surface by means of etching and chemical reactions. Fig. 8 shows the FESEM micrographs of control and DC air plasma treated samples and the extent of etching has been quantified by calculating mean pore radius (Table 11).

As per the modified Lucas Washburn equation an increase in mean pore radius improves capillarity action thereby enhancing the hydrophilicity of the fabric.

ATR-FTIR analysis was carried out on specific regions of all fifteen samples before and after plasma treatment to analyse the chemical reactions. The Lateral Order Index (LOI) (i.e) the absorbance ratio between peaks in the range 1420–1430 cm^{-1} (CH_2 scissoring in the crystalline region) and peak corresponding to 898 cm^{-1} (glycosidic C–*O*–C in the amorphous region) proposed by Nelson and O'Connor [9] is calculated using IR data. The LOI value delivers the information related to lateral ordering of cellulose chains and the intensity difference in the carbonyl and carboxyl group gives information about the functionalisation of cellulose. The following general conclusions can be drawn the data. The LOI value decreases after plasma treatment for all the samples thus promoting amorphicity and inturn produces free hydroxyl groups which is naturally hydrophilic and the appearance of peak in the range between 1710 and 1720 cm^{-1} after plasma treatment confirms the oxidation of sample, thus improving the polar nature of sample and hence hydrophilicity. The effect of variation in ion density with pressure and hence its effect on etching and chemical modification induced on the fabric surface is as follows: Firstly, it can be inferred that the decrease in mean free path with pressure decreases the effective surface etching and leads to a depreciation in the capillary action. Secondly, for all the combinations of current and time, at low pressure the extent of decrease in LOI increases with pressure thus leading to the generation of more free hydroxyl group whereas at high pressure, extent of decrease in LOI decreases hence there is a decrease in hydrophilicity with increase in pressure. Similarly, the oxidation process is dominant at low pressure which is evident from the intensity of carbonyl and carboxyl groups (Fig. 9 and Table 12).

The synergetic effect of both the process is the reason for the decrease in hydrophilicity with increase in pressure.

Fig. 5(b) gives the relationship between DC current and wicking height for different combinations of pressure and time. It is from Table 10 that wicking height increases with increase in DC current and saturates beyond approximately 35 mA. The Langmuir probe study (Table 10) shows that the ion density increases and electron energy decreases with increase in current for all the combinations of gas pressure and exposure time. This is attributed to an efficient energy transfer from electron to the plasma species due to inelastic collisions [24] which in turn increases the generation of ions. The generated ions with enhanced kinetic energy has a greater penetration depth due to increased electric field thus accounting for an increase in hydrophilicity [23]. The calculated LOI using the ATR-FTIR spectral data from Table 11 shows that higher ion density

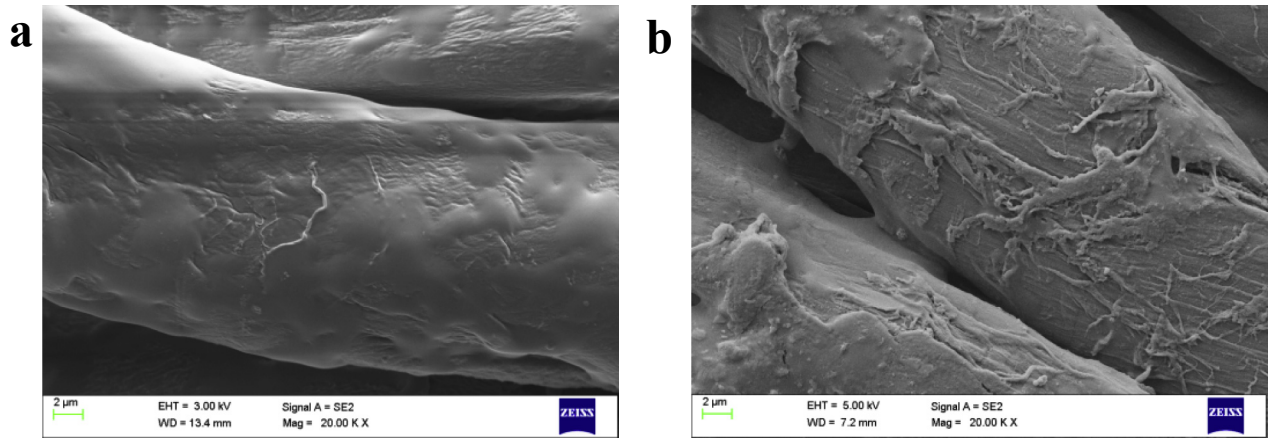

Fig. 8. FESEM micrographs of a) Control and b) DC air plasma treated fabric.

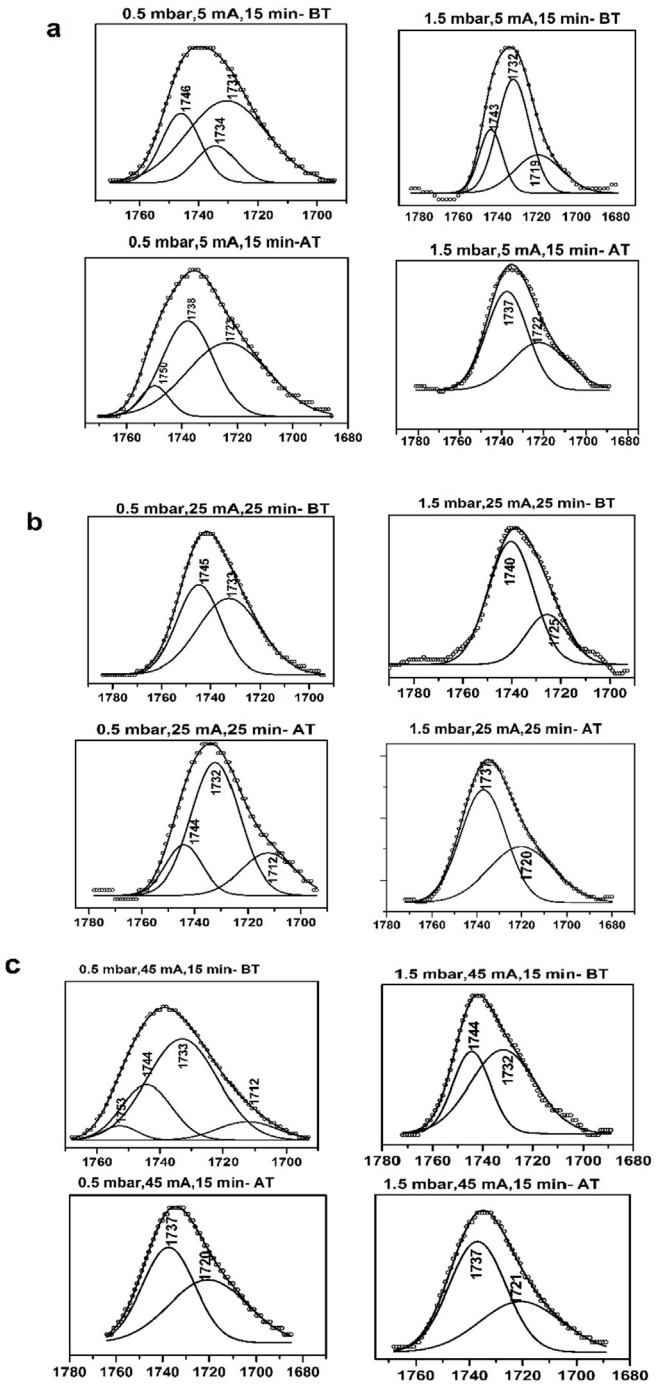

Fig. 9. Deconvolution of C-O and C=O peaks of DC air plasma treated samples (pressure variation).

with increased kinetic energy upon interaction with the fabric surface increases the amorphicity of the sample thus leading to a higher concentration of free hydroxyl groups. Also, the increase in absorption coefficient of peaks pertaining to aldehyde C=O stretching and the appearance of peaks corresponding to carboxylic acid C=O stretching (Fig. 10 and Table 12) confirms the oxidation of primary alcohol and the aldehyde respectively. The generation of free hydroxyl groups and subsequent oxidation of cellulose sample, synergitically enhances the polar nature of fabric thus improving hydrophilicity. However, for a combination of 1 mbar gas pressure and 5 min exposure time the oxidation process dominates the crystallinity effect. Simultaneously, the capillary action of the fiber is promoted by an increase in mean pore radius with DC current.

Fig. 5(c) explains the variation of wicking height with plasma exposure time for fixed combinations of gas pressure and DC current. The ion density is dependent on process gas pressure and DC current. Hence, for a combination of high DC current and low gas pressure shown in Table 10, the variation in wicking height is not so significant denoting that the effective modification happens almost during the initial stages of plasma treatment. For other two combinations of gas pressure and DC current, though the ion density remains same with time the continuous collision among the charged particles in the plasma zone could possibly lead to a decrease in this energy due to inelastic collisions, thus resulting in a comparitively impeded physical and chemical modification on the surface which is evident from Table 10. Hence, the hydrophilicity decreases with time. The variation in mean pore radius, LOI and extent of oxidation (Fig. 11) has been analyzed and discussed. For both the regions the etching effect increases the generation of fibrils which inturn closing the existing pore on the fibers thus reducing the hydrophilicity. As far as mid pressure is concerned, while comparing the lower treatment time though the extent of amorphous nature has been increased due to the reduction of LOI after plasma treatment effective oxidation has not occurred, hence the hydrophilicity is closer to the control sample. Whereas in the case of high pressure, it is clear that extent of oxidation has been improved (Fig. 11) increasing the hydrophilicity when compared to the untreated sample. However, the reduced capillary action with increase in time impairs the hydrophilicity when compared to lower treatment.

Fig. 6(a) depicts that a simultaneous variation in gas pressure and plasma exposure time from a low to high value for a fixed DC current suppresses the hydrophilicity. This is attributed to the reduced mean free path that impairs the effective fabric surface modification. Fig. 6(b) reveals an enhancement in hydrophilicity of the plasma treated fabric with simultaneous increase in DC current and exposure time for a fixed gas pressure. This is attributed to the increase in ion density due to inelastic collision with energetic electrons which is a result of higher electric field existing between the electrodes and hence an effective surface modification.

3.5. Optimisation of process parameters

The optimisation is performed to achieve the maximum hydrophilicity of the DC plasma treated samples for the selected range of parameters. The suitability of model equations for predicting the maximum response values is tested using selected optimal conditions. By applying the desirability function method in response surface methodology, thirty solutions are obtained with desirability 1. The optimum values of the process conditions for DC air plasma treatment is obtained for a combination of gas pressure: 0.5 mbar, time of treatment: 15 min and DC current: 25 mA. The wicking response obtained experimentally is 12.6 cm while theoretical value is 13.1 cm. The result of the analysis confirm that the quadratic equation generated by the model governs the DC plasma process within the mention operating range.

4. Conclusions

Optimisation of the process parameters involved in the plasma surface modification of cotton fabric to achieve maximum wicking response using Box-Behnken design disclosed the fact that the

Table 12
Intensity of carboxyl and carbonyl peaks of process parameters.

Pressure variation										
I (mA)	T (min)	P (mbar)	WH (cm)	Intensity of C=O stretching							
				Aldehyde				Acid			
				BT		AT		BT		AT	
				WN (cm^{-1})	Intensity	WN (cm^{-1})	Intensity	WN (cm^{-1})	Intensity	WN (cm^{-1})	Intensity
5	15	0.5	11.28	1746	5.49E-4	1750	1.95E-4	_	_	1723	4.60E-4
				1738	2.33E-4	1738	5.97E-4				
				1730	5.09E-4						
5	15	1.5	10.50	1743	7.42E-4	1737	1.59E-3	1719	4.42E-4	1722	7.60E-4
				1732	1.34E-3						
25	25	0.5	13.13	1745	9.15E-4	1744	2.16E-4	_	_	1712	1.75E-4
				1733	7.63E-4	1732	6.07E-4				
25	25	1.5	11.80	1741	2.03E-3	1737	1.81E-3	1726	8.20E-4	1720	8.77E-4
45	15	0.5	13.34	1753	0.094	1737	6.25E-4	_	_	1720	4.02E-4
				1744	6.62E-4					1712	2.25E-4
				1733	1.21E-4						
45	15	1.5	12.90	1744	7.15E-4	1737	1.04E-3	_	_	1721	6.49E-4
				1732	7.35E-4						

Current variation											
P (mbar)	**T (min)**	**I (mA)**	**WH (cm)**	**Intensity of C=O stretching**							
				Aldehyde				**Acid**			
				BT		**AT**		**BT**		**AT**	
				WN (cm^{-1})	**Intensity**	**WN (cm^{-1})**	**Intensity**	**WN (cm^{-1})**	**Intensity**	**WN (cm^{-1})**	**Intensity**
0.5	15	5	11.28	1746	5.49E-4	1750	1.95E-4	_	_	1723	4.60E-4
				1738	2.33E-4	1738	5.97E-4				
				1730	5.09E-4						
0.5	15	45	13.34	1753	0.094	1737	6.25E-4	_	_	_	4.02E-4
				1744	6.62E-4						2.25E-4
				1733	1.21E-4						
1	5	5	11.26	1740	1.17E-3	1744	1.12E-3	_	_	_	8.90E-4
				1729	1.42E-3	1733	6.50E-4				
1	5	45	12.30	1747	2.57E-4	1749	4.40E-4	_	_	_	9.00E-4
				1740	1.25E-4	1737	1.46E-3				
				1733	7.59E-4						
1.5	15	5	10.50	1743	7.42E-4	1737	1.59E-3	1719	4.42E-4	1722	7.60E-4
				1732	1.34E-3						
1.5	15	45	12.90	1744	7.15E-4	1737	1.04E-3	–		1721	6.49E-4
				1732	7.35E-4						

Time variation											
I (mA)	**P (mbar)**	**T (min)**	**WH (cm)**	**Intensity of C=O stretching**							
				Aldehyde				**Acid**			
				BT		**AT**		**BT**		**AT**	
				WN (cm^{-1})	**Intensity**	**WN (cm^{-1})**	**Intensity**	**WN (cm^{-1})**	**Intensity**	**WN (cm^{-1})**	**Intensity**
25	0.5	5	12.94	1743	1.34E-4	1743	1.29E-4	_	_	_	2.83E-4
				1734	5.80E-4	1734	3.09E-4				
25	0.5	25	13.13	1745	9.15E-4	1744	2.16E-4	_	_	_	1.75E-4
				1733	7.63E-4	1732	6.07E-4				
5	1	5	11.26	1740	1.17E-3	1744	1.12E-3	_	_	_	8.90E-4
				1729	1.42E-3	1733	6.50E-4				
5	1	25	9.46	1740	1.44E-3	1738	8.23E-4	1725	9.09E-4	1722	5.05E-4
								1710	2.66E-4		
25	1.5	5	13.30	1740	1.78E-3	1742	2.27E-3	1726	1.22E-3	1728	2.28E-3
								1710	4.18E-4	1710	6.10E-4
25	1.5	25	11.80	1741	2.03E-3	1737	1.81E-3	1726	8.20E-4	1720	8.77E-4

equation that governs the process is quadratic in nature. The ANOVA of the design parameters revealed that the variation in individual parameters namely gas(commercial grade air) pressure, DC current and process time while maintaining other two parameters as constant and interaction effect of gas pressure & exposure time and DC current & exposure time had an influence on the hydrophilicity of the fabric. The single Langmuir probe analysis of DC air plasma with in the operating range chosen depicted an increase in ion density with increase in gas pressure. The effect of reduced mean free path lead to a decline in the effectiveness of surface modification which reflected as a decrease in LOI, extent of oxidation and mean pore radius and hence the hydrophilicity. Further, increase in ion density due to inelastic energy transfer through electron collision with an increase in DC current resulted in

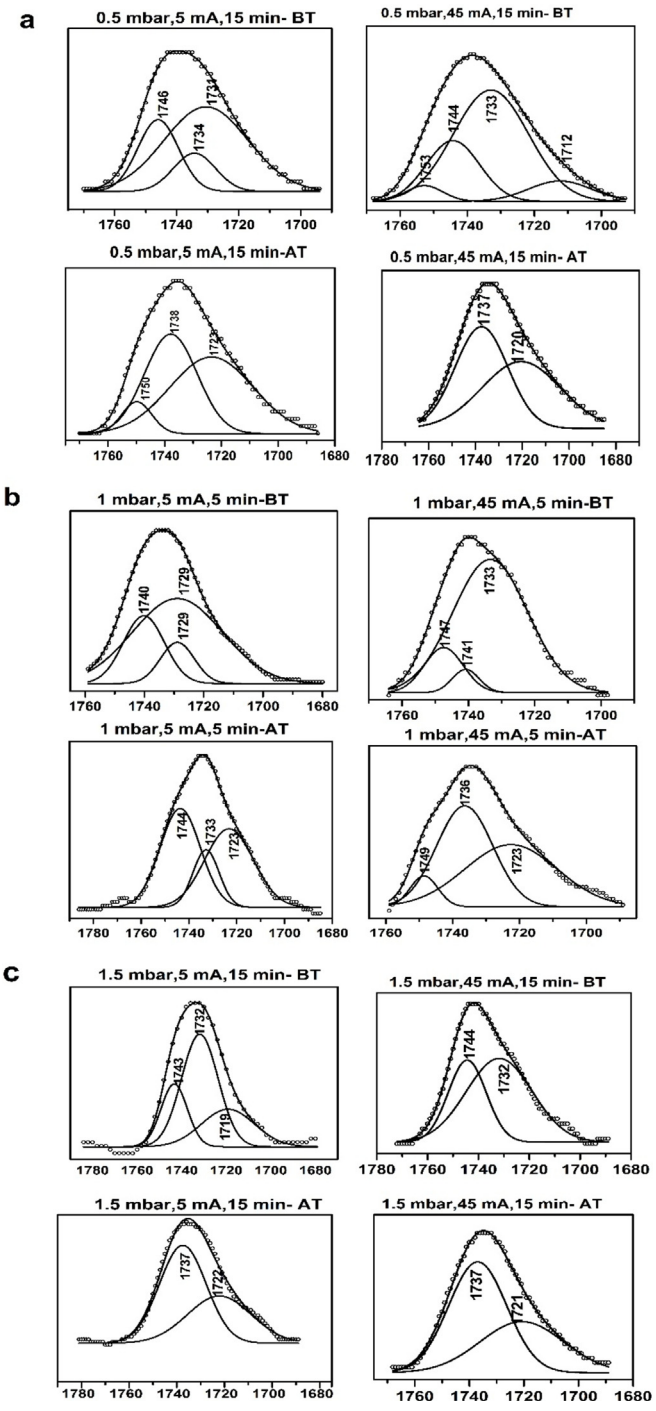

Fig. 10. Deconvolution of C-O and C=O peaks of DC air plasma treated samples (current variation).

effective physical and chemical modification thus improving the wicking response with DC current. It was also observed that effective modification of the fabric surface was almost complete within 5 min of fabric's exposure and subsequent exposure of upto 25 min lead to inelastic collisions among the plasma species thereby impeding effective surface modification. Error analysis showed the experimental (actual) and predicted response was linear affirming that the quadratic equation suggested by the design perfectly governs the process.

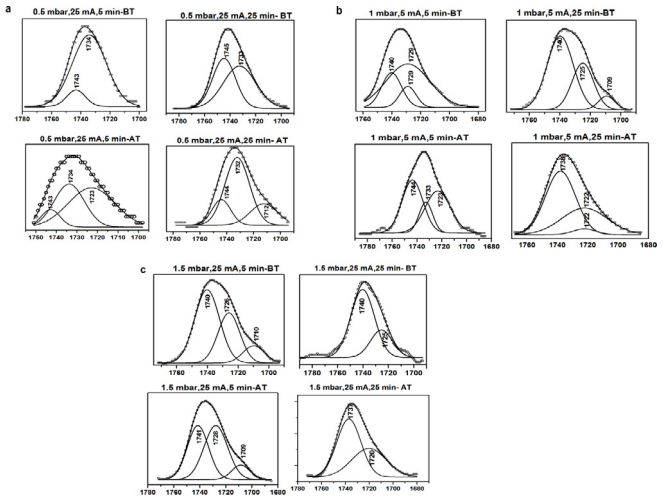

Fig. 11. Deconvolution of C-O and C=O peaks of DC air plasma treated samples (time variation).

Acknowledgements

The authors wish to thank the Management and Principal, PSG College of Technology, Coimbatore for providing the necessary infrastructure to carry out the study.

References

[1] Baghery Borooj Meysam, Mousavi Shoushtari Ahmad, Haji Aminoddin, et al., Optimization of plasma treatment variables for the improvement of carbon fibres/epoxy composite performance by response surface methodology Composites, Sci. Technol. 128 (2016) 215–221.
[2] D.L. Massart, B.G.M. Vandeginste, L.M.C. Buydens etal, Handbook of Chemometrics and Quali-metrics Part A, Elsevier, Amsterdam, 2003.
[3] B.B. Neto, I.M. Scarminio, R.E. Bruns, How Do Experiments: Research and Development in Science and Industry. Research and Development in Science and Industry, Campinas, Oxford University Press, 2003.
[4] S.L.C. Ferreira, W.N.L. dos Santos, C.M. Quintella, etal, Doehlert Matrix: a chemometric toll for analytical chemistry—review, Talanta 63 (2004) 1061–1067.
[5] Dipayan Das, Rashmi Thakur, Arun Kumar Pradhan, Optimization of corona discharge process using Box Behnken design of experiments, J. Electrost. 70 (2012) 469–473.
[6] Pandurangan Senthilkumar, Thangavelu Karthik, Effect of argon plasma treatment variables on wettability and antibacterial properties of polyester fabrics, J. Inst. Eng. India Ser. E (2015), https://doi.org/10.1007/s40034-015-0074-0.
[7] T. Karthik, R. Murugan, M. Vijayan, Optimization of plasma treatment variables to improve the hydrophilicity of polylinen fabrics, J. Textil. Inst. 104 (No. 5) (2013) 481–493.
[8] M. Prabhakaran, N. Carneiro, Effect of low temperature plasma on cotton fabric and its applications to bleaching and dyeing, Indian J. Fibre Text. Res. 30 (2005) 68–74.
[9] M.L. Nelson, R.T. O'Connor, Relation of certain infrared bands to cellulose crystallinity and crystal lattice type. Part I. Spectra of types I, II, III and of amorphous cellulose, J. Appl. Polym. Sci. 8 (1964) 1311–1324.
[10] Robert T. O'Connor, Elsie F. DuPré, Donald Mitcham, Cottons: Part I: physical and crystalline modifications and oxidation, Textil. Res. J. 28 (1958) 382, https://doi.org/10.1177/004051755802800503.
[11] G.E.P. Box, D.W. Behnken, Technometrics, Some New Three Level Designs for the Study of Quantitative Variables, 1960.
[12] Method of Test for Wettability of Textile Fabrics, BSI, 20 February 1970.
[13] V.I. Demidov, S.V. Ratynskaia, K. Rypdal, Electric probes for plasmas: the link between theory and instrument, Rev. Sci. Instrum. 73 (2002) 3409–3439.
[14] F.F. Chen, R.H. Huddlestone, S.L. Leonard, in: Electric Probes. Plasma Diagnostic Techniques, Academic Press, New York, 1965.
[15] E.P. Kalogianni, T. Savopoulos, T.D. Karapantsios, S.N. Raphaelides, A dynamic wicking technique for determining the effective pore radius of pregelatinized starch sheets, Colloids Surf. B: Biointerfaces 35 (2004) 159–167.
[16] Pengpeng Qiu, Mingcan Cui, Kyounglim Kang, et al., Application of Box–Behnken design with response surface methodology for modelling and optimizing ultrasonic oxidation of arsenite with H2O2,methodology for modelling and optimizing ultrasonic oxidation of arsenite with H2O2, Cent. Eur. J. Chem. 12 (2014) 164–172.

[17] R. Minjares-Fuentes, A. Femenia, Garau MC. etal, Ultrasound-assisted extraction of pectins from grape pomace using citric acid: a response surface methodology approach Carbohydrate, Polymers 106 (2014) 179–189.
[18] G.A. Lewis, Encyclopedia of Pharmaceutical Technology, second ed., Marcel Dekker, New York, 2002, pp. 1922–1937.
[19] Sukhbir Singh, Yash Paul Singla, Sandeep Arora, Statistical, Diagnostic and response surface analysis of nefopam hydrochloride nanospheres using 35 Box-Behnken design, Int. J. Pharm. Pharmaceut. Sci. 7 (2015) 89–101.
[20] Issac D. Sudit, R. Claude Woods, A study of the accuracy of various Langmuir probe theories, J. Appl. Phys. 76 (1994) 4489–4498.
[21] Alexandre A. Radzig, Boris M. Smirnov, Reference Data on Atoms, Molecules,and Ions, in: Springer Series in Chemical Physics, Springer-Verlag, Berlin Heidelberg New York Tokyo, 1985.
[22] K.H. Becker, K. Kogelschatz, K.H. Schoenbach, et al., Non-equilibrium Air Plasmas at Atmospheric Pressure, IOP publishing Ltd, Bristol, UK, 2005.
[23] H.U. Poll, U. Schladitz, S. Schreiter, Penetration of plasma effects into textile structures, Surf. Coating. Technol. 142–144 (2001) 489–493.
[24] Brian Chapman, Glow Discharge Processes: Sputtering and Plasma Etching, Wiley publications, USA, 1980.